doi:10.1246/cl.2011.72

Assembly Structures and Spin Crossover Properties of Facial and Meridional Isomers of Tris[benzyl(2-methylimidazol-4-ylmethylidene)amine]iron(II) Chloride Hexafluorophosphate

Daisuke Furusho,[1] Koshiro Nishi,[1] Tomotaka Hashibe,[1] Takeshi Fujinami,[1] Hiroaki Hagiwara,[1] Naohide Matsumoto,*[1]
Malcolm A. Halcrow,[2] Seiichiro Iijima,[3] Yukinari Sunatsuki,[4] and Masaaki Kojima[4]
[1]*Department of Chemistry, Faculty of Science, Kumamoto University, 2-39-1 Kurokami, Kumamoto 860-8555*
[2]*School of Chemistry, University of Leeds, Woodhouse Lane, Leeds LS2 9JT, UK*
[3]*National Institute of Advanced Industrial Science and Technology, Tsukuba, Ibaraki 305-8566*
[4]*Department of Chemistry, Faculty of Science, Okayama University, 3-1-1 Tsushima-naka, Okayama 700-8530*

(Received October 7, 2010; CL-100858; E-mail: naohide@aster.sci.kumamoto-u.ac.jp)

Facial- and *meridional*-isomers of tris[benzyl(2-methylimidazol-4-ylmethylidene)amine]iron(II) chloride hexafluorophosphate with the formulas of *fac*-$[Fe(HL^{Me\text{-}Benz})_3]Cl\cdot PF_6\cdot EtOH\cdot H_2O$ (**1**) and *mer*-$[Fe(HL^{Me\text{-}Benz})_3]Cl\cdot PF_6\cdot 1.5H_2O$ (**2**) were selectively crystallized in ethanol and methanol, respectively. All three imidazole groups in both the *fac*- and *mer*-$[Fe(HL^{Me\text{-}Benz})_3]^{2+}$ cations are hydrogen-bonded to neighboring Cl^- ions and give the assembly structures. The compounds differ, however, in that **1** has a discrete cubane-like tetranuclear cluster, while **2** forms a two-dimensional (2D) network structure. The magnetic susceptibilities data revealed that **1** and **2** are spin crossover complexes.

Spin crossover (SCO) iron(II) complex exhibits a molecular bistablity in which the electronic configuration changes between high-spin ($S = 2$) and low-spin ($S = 0$) states by external perturbations, such as temperature, light, and pressure, leading to distinctive changes in molecular geometry, color, and magnetism.[1] While SCO is a phenomenon of a single molecule, the forms of the SCO properties such as steep, multistep SCO, hysteresis, and LIESST (light-induced excited spin state trapping) are brought from the cooperative effect among SCO molecules. Therefore SCO complexes exhibiting intermolecular interaction or/and network structure have attracted much attention. The latest SCO studies demonstrate that strong covalent bonding between SCO sites does not always afford cooperative switching, while weak intermolecular interactions such as hydrogen bond and π–π stacking often provide “effective cooperatives” to afford valuable SCO properties in a crystalline lattice.[2]

We have shown that metal complexes of polydentate ligands involving imidazole groups give a variety of aggregated assembly structures due to the imidazole–imidazolate and imidazole–halogen hydrogen bonds.[3] Further iron compounds exhibit interesting SCO properties such as steep, multistep SCO, hysteresis, chiral aggregation, and mixed-valence states.[4] These studies demonstrate that iron complexes of imidazole-containing ligands have advantages in designing the assembly structures and in tuning the spin crossover region of the ligand field strength. In this study, we studied the Fe^{II} complex of new bidentate ligand benzyl(2-methylimidazol-4-ylmethylidene)amine, where the bidentate ligand abbreviated as $HL^{Me\text{-}Benz}$ is the 1:1 condensation product of 2-methyl-4-formylimidazole and benzylamine. By using the different reaction solvents, we obtained two types of crystals, *facial*- and *meridional*-forms of tris[benzyl(2-methylimidazol-4-ylmethylidene)amine]iron(II) chloride hexafluorophosphate, *fac*-$[Fe(HL^{Me\text{-}Benz})_3]Cl\cdot PF_6\cdot EtOH\cdot H_2O$ (**1**) and *mer*-$[Fe(HL^{Me\text{-}Benz})_3]Cl\cdot PF_6\cdot 1.5H_2O$ (**2**). The X-ray analyses of **1** and **2** revealed not only the *facial* and *meridional* isomerism but also two different assembly structures generated from the same motif of the imidazole–chloride hydrogen bond, that is, a cubane-like tetranuclear structure in **1** and a 2D network structure in **2**. We report here their syntheses, their interesting assembly structures, and spin crossover behavior.

The reaction solvent is the key for the selective syntheses of *fac*- and *mer*-isomers **1** and **2**. All the synthetic procedures were performed in air. The complex *fac*-$[Fe(HL^{Me\text{-}Benz})_3]Cl\cdot PF_6\cdot EtOH\cdot H_2O$ (**1**) was prepared in ethanol.[5] The ligand was prepared by the 1:1 condensation reaction of 2-methyl-4-formylimidazole and benzylamine in ethanol. To the resultant ethanol solution of the ligand was added an ethanol solution of $FeCl_2\cdot 4H_2O$, and then that of $NaPF_6$ with a 3:1:1 molar ratio. The mixture was stirred for 1 h at room temperature, and then filtered. The filtrate was left to stand for a few days in a refrigerator, during which time large pale yellow cubic crystals precipitated. The complex *mer*-$[Fe(HL^{Me\text{-}Benz})_3]Cl\cdot PF_6\cdot 1.5H_2O$ (**2**) was prepared by a similar way to **1**, where methanol instead of ethanol was used as the reaction solvent.[6] During the crystallization of **2** in methanol, yellow colored crystals of **2** with a very small amount of red crystals precipitated. Red crystals were removed manually and the yellow crystals were subjected to physical measurements. The yellow complex was later confirmed to be *mer*-$[Fe(HL^{Me\text{-}Benz})_3]Cl\cdot PF_6\cdot 1.5H_2O$ (**2**).

The C, H, and N elemental analyses of **1** and **2** suggested the existence of lattice solvents. The presence of such solvent was examined by TGA (thermogravimetric analysis). The samples were heated from room temperature to 160 °C and then cooled from 160 °C to room temperature at the heating rate of $2\,°C\,min^{-1}$. A continuous weight loss of 7.1% corresponding to $EtOH + H_2O$ for **1** was observed in the heating mode. A weight loss of 3.1% corresponding to $1.5H_2O$ for **2** was observed in heating mode and a weight increase of $0.5H_2O$ was observed in the subsequent cooling mode measurement. Both complexes showed a thermochromism in the solid states from yellow at ambient temperature to dark red at liquid nitrogen temperature, suggesting SCO.

The crystal structures of **1** and **2** were determined by single-crystal X-ray diffraction analyses at 296 K.[5,6] Complex **1** crystallizes in a cubic space group $P\bar{4}3n$ (no. 218) with the general positions of $Z = 24$. The unit cell contains eight formula units $[Fe(HL^{Me\text{-}Benz})_3]Cl\cdot PF_6\cdot EtOH\cdot H_2O$ so that one third of the formula is a crystallographic unique unit, consisting of one

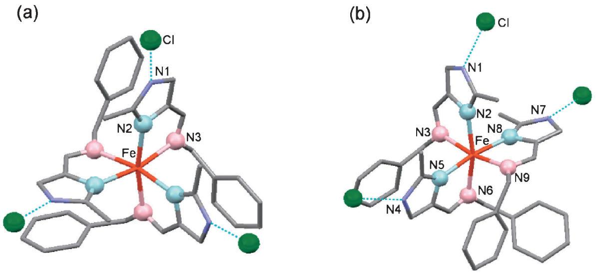

Figure 1. (a) Molecular structure of the complex cation of **1** with the selected atom numbering scheme viewed along C_3 axis, showing *fac*-$[\mathrm{Fe(HL^{Me\text{-}Benz})_3}]^{2+}$ isomer. (b) Molecular structure of the complex cation of **2** with the selected atom numbering scheme, showing *mer*-$[\mathrm{Fe(HL^{Me\text{-}Benz})_3}]^{2+}$ isomer. Three imidazole groups per complex cation in both compounds are hydrogen-bonded to three neighboring $\mathrm{Cl^-}$ ions (green).

ligand $\mathrm{HL^{Me\text{-}Benz}}$ at the general position, Fe and Cl atoms positioned at their threefold rotation axis, and two crystallographically different $\mathrm{PF_6}^-$ ions. One of the two $\mathrm{PF_6}^-$ ions is positioned at the fourfold rotation axis and the other spans threefold and twofold rotation axes. Complex **2** crystallizes in a monoclinic space group $P2_1/c$ (no. 14) with $Z = 4$. The crystallographic unique unit consists of one complex cation $[\mathrm{Fe(HL^{Me\text{-}Benz})_3}]^{2+}$, one chloride ion, one hexafluorophosphate ion, and $1.5\mathrm{H_2O}$.

Figures 1a and 1b show the molecular structures of the complex-cation parts $[\mathrm{Fe(HL^{Me\text{-}Benz})_3}]^{2+}$ and three neighboring hydrogen-bonded $\mathrm{Cl^-}$ ions of **1** and **2** with their selected atom numbering schemes, respectively. Each $\mathrm{Fe^{II}}$ ion for both complexes is octahedrally coordinated by the $\mathrm{N_6}$ donor atoms of three bidentate $\mathrm{HL^{Me\text{-}Benz}}$ ligands. Of the two possible geometrical isomers, the complexes **1** and **2** take the *fac*- and *mer*-isomer, respectively. On the basis of the Fe–N bond distances and N–Fe–N bond angles, the spin state of the complexes at 296 K can be identified. At 296 K, the Fe–N distances are in the range of 2.194(3)–2.221(3) and 2.136(5)–2.242(5) Å for **1** and **2**, respectively, which is typical for HS $\mathrm{Fe^{II}}$ bound to $\mathrm{N_6}$ donors.

All three imidazole groups in both the *fac*- and *mer*-$[\mathrm{Fe(HL^{Me\text{-}Benz})_3}]^{2+}$ cations in **1** and **2** are hydrogen-bonded to neighboring $\mathrm{Cl^-}$ ions. For **1**, the three imidazole–chloride hydrogen bonds are equivalent, and the hydrogen bond distance is $\mathrm{N(1)\cdots Cl^-} = 3.123(5)$ Å. For **2**, three hydrogen bond distances are $\mathrm{N(1)\cdots Cl^-} = 3.162(7)$ Å, $\mathrm{N(4)\cdots Cl^-} = 3.067(8)$ Å, and $\mathrm{N(7)\cdots Cl^-} = 3.182(9)$ Å. Although imidazole–chloride hydrogen bonding is a common motif for the construction of assembly structures, very different structures are generated for **1** and **2**, as easily imagined by the directions of the three $\mathrm{NH\cdots Cl^-}$ interactions in Figure 1.

Complex **1** forms a tetrameric cubane-like structure. Figure 2a shows the cubane structure of $\{$*fac*-$[\mathrm{Fe(HL^{Me\text{-}Benz})_3}]^{2+}\cdots\mathrm{Cl^-}\}_4$ constructed from twelve $\mathrm{NH\cdots Cl^-}$ hydrogen bonds. The cubane encapsulates a $\mathrm{PF_6}^-$ anion which is subjected to a disorder probably due to free rotation at 296 K. Another $\mathrm{PF_6}^-$ ion occupies the space among the cubane-like molecules and shows no disorder even at 296 K. The *fac*-$[\mathrm{Fe(HL^{Me\text{-}Benz})_3}]^{2+}$ cation is a chiral species with two enantiomorphs *fac*-Δ-$[\mathrm{Fe(HL^{Me\text{-}Benz})_3}]^{2+}$ and *fac*-Λ-$[\mathrm{Fe(HL^{Me\text{-}Benz})_3}]^{2+}$.

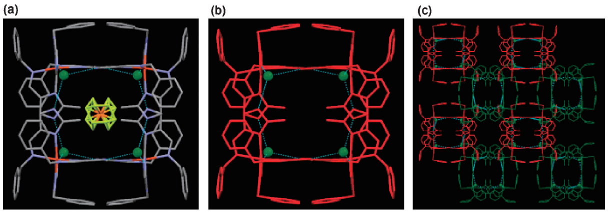

Figure 2. (a) The cubane-like tetranuclear structure of **1** constructed from twelve $\mathrm{NH\cdots Cl^-}$ hydrogen bonds, where a $\mathrm{PF_6}^-$ anion is encapsulated in the center of the cubane. The encapsulated $\mathrm{PF_6}^-$ ion is subjected to disorder probably due to free rotation at 296 K. (b) Homochiral cubane-like tetranuclear cluster of **1**, consisting of four *fac*-Λ-$[\mathrm{Fe(HL^{Me\text{-}Benz})_3}]^{2+}$ species (red colored). (c) Packing diagram of **1**. In a crystal lattice, homochiral cubane-like tetramers with the opposite chiralities (red *fac*-Λ-$[\mathrm{Fe(HL^{Me\text{-}Benz})_3}]^{2+}$ and green *fac*-Δ-$[\mathrm{Fe(HL^{Me\text{-}Benz})_3}]^{2+}$) are arrayed alternately.

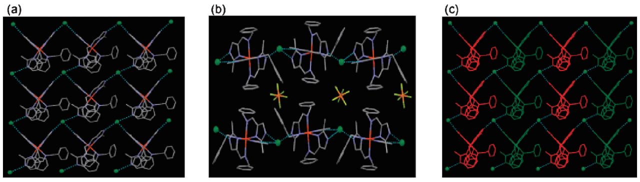

Figure 3. (a) Three imidazole groups per a complex-cation of *mer*-$[\mathrm{Fe(HL^{Me\text{-}Benz})_3}]^{2+}$ are hydrogen-bonded to three neighboring $\mathrm{Cl^-}$ ions by $\mathrm{NH\cdots Cl^-}$ hydrogen-bonds to produce a hydrogen-bonded two-dimensional network structure, in which the net unit is a cyclic trimer $\{$*mer*-$[\mathrm{Fe(HL^{Me\text{-}Benz})_3}]^{2+}\cdots\mathrm{Cl^-}\}_3$. (b) Side view of the adjacent layers, showing the layer is not undulated and $\mathrm{PF_6}^-$ counter anions occupy the space between the layers. (c) Hetero-chiral 2D layer. The *mer*-$[\mathrm{Fe(HL^{Me\text{-}Benz})_3}]^{2+}$ cation is also a chiral species with two possible optical isomers *mer*-Δ-$[\mathrm{Fe(HL^{Me\text{-}Benz})_3}]^{2+}$ and *mer*-Λ-$[\mathrm{Fe(HL^{Me\text{-}Benz})_3}]^{2+}$. Two enantiomorphs are drawn by red and green colors.

It should be noted that a cubane-like tetranuclear structure is built up by homochiral four *fac*-Δ-$[\mathrm{Fe(HL^{Me\text{-}Benz})_3}]^{2+}$ or four *fac*-Λ-$[\mathrm{Fe(HL^{Me\text{-}Benz})_3}]^{2+}$. Figure 2b shows a homochiral tetranuclear structure, where the red colored molecule indicates the *fac*-Λ-$[\mathrm{Fe(HL^{Me\text{-}Benz})_3}]^{2+}$ isomer. In the crystal lattice, homochiral cubane-like tetramers with the opposite chiralities (red *fac*-Λ-$[\mathrm{Fe(HL^{Me\text{-}Benz})_3}]^{2+}$ isomer and green *fac*-Δ-$[\mathrm{Fe(HL^{Me\text{-}Benz})_3}]^{2+}$) are arrayed alternately, as shown in Figure 2c.

As shown in Figure 3a, the three imidazole nitrogen atoms of the *mer*-$[\mathrm{Fe(HL^{Me\text{-}Benz})_3}]^{2+}$ cation in **2** are hydrogen-bonded to their three neighboring $\mathrm{Cl^-}$ ions to form a two-dimensional network structure, in which the repeating unit is a cyclic trimer $\{[\mathrm{Fe(HL^{Me\text{-}Benz})_3}]^{2+}\cdots\mathrm{Cl^-}\}_3$. Figure 3b shows a side view of the adjacent layers, presenting that the layer is not undulated and $\mathrm{PF_6}^-$ counter anions occupy the space between the layers. The *mer*-$[\mathrm{Fe(HL^{Me\text{-}Benz})_3}]^{2+}$ cation is also a chiral species with two possible enantiomorphs *mer*-Δ-$[\mathrm{Fe(HL^{Me\text{-}Benz})_3}]^{2+}$ and *mer*-Λ-$[\mathrm{Fe(HL^{Me\text{-}Benz})_3}]^{2+}$. As shown in Figure 3c, each layer in **2** consists of two enantiomorphs, giving a hetero-chiral 2D network structure.

The magnetic susceptibilities for the ground samples were measured upon cooling from 300 to 5 K and then remeasured upon warming from 5 to 300 K at 2 K min^{-1} under a 0.5 T applied magnetic field by the use of a SQUID magnetometer. The $\chi_M T$ vs. T plots are shown in Figure 4, where χ_M is the

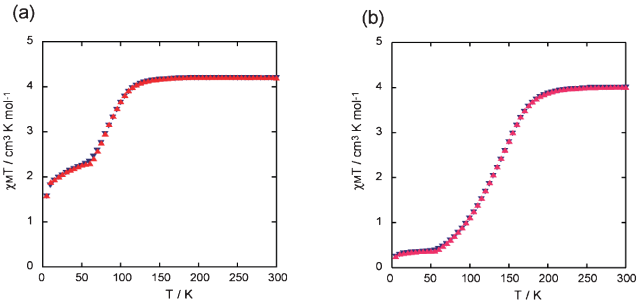

Figure 4. SCO behaviors of *fac*-[Fe(HL$^{\text{Me-Benz}}$)$_3$]Cl$\cdot$PF$_6$$\cdot$EtOH$\cdot$H$_2$O (**1**) and *mer*-[Fe(HL$^{\text{Me-Benz}}$)$_3$]Cl$\cdot$PF$_6$$\cdot$1.5H$_2$O (**2**), in the form of $\chi_M T$ per Fe versus T plots.

molar magnetic susceptibility per Fe and T is the absolute temperature.

The $\chi_M T$ vs. T plots of *fac*-[Fe(HL$^{\text{Me-Benz}}$)$_3$]Cl$\cdot$PF$_6$$\cdot$EtOH$\cdot$H$_2$O (**1**) showed an incomplete SCO behavior. At temperatures higher than 120 K, the constant $\chi_M T$ value of ca. 4.2 cm^3 K mol^{-1} per iron atom is a little higher than the spin-only HS Fe$^{\text{II}}$ value and is compatible with reported HS Fe$^{\text{II}}$ ($S = 2$) complexes. On lowering the temperature, the $\chi_M T$ value decreases from the constant value of 4.2 to 2.1 cm^3 K mol^{-1} at 50 K, which is half the HS value. This indicates that the spin transition occurs from 4HS state of tetrameric Fe$_4$ molecule to 2HS + 2LS. Calculation of the derivative of d($\chi_M T$)/dT vs. T evaluated the spin transition temperature $T_{1/2} = 80$ K between 4HS state and 2HS + 2LS state.

The $\chi_M T$ vs. T plots of *mer*-[Fe(HL$^{\text{Me-Benz}}$)$_3$]Cl$\cdot$PF$_6$$\cdot$1.5H$_2$O (**2**) showed SCO behavior. At temperatures higher than 200 K, the constant $\chi_M T$ value of ca. 4.0 cm^3 K mol^{-1} is the value reported for the HS Fe$^{\text{II}}$ ($S = 2$) complexes. At temperatures lower than 50 K, a plateau value of nearly 0.3 cm^3 K mol^{-1} is a little larger than the theoretical value of LS Fe$^{\text{II}}$ ($S = 0$) and is compatible with the reported values for LS Fe$^{\text{II}}$ ($S = 0$) complexes. In the wide temperature region of 60–180 K, the $\chi_M T$ value changes gradually between the HS and LS values. The SCO curve is a little shifted from the ideal one-step SCO behavior.

In this study, *facial* and *meridional* isomers *fac*-[Fe(HL$^{\text{Me-Benz}}$)$_3$]Cl$\cdot$PF$_6$$\cdot$EtOH$\cdot$H$_2$O (**1**) and *mer*-[Fe(HL$^{\text{Me-Benz}}$)$_3$]Cl$\cdot$PF$_6$$\cdot$1.5H$_2$O (**2**) have been selectively synthesized by using different reaction solvents, tris[benzyl(2-methylimidazol-4-ylmethylidene)amine]iron(II) complex can give not only *fac*- and *mer*-geometric isomers but also Δ- and Λ-optical isomers. Further, the imidazole groups of a complex-cation can act as a functional group to form assembly structures by hydrogen bonding. In fact, all three imidazole groups per complex are hydrogen-bonded to three neighboring Cl$^-$ ions to form a discrete cubane-like tetranuclear structure in **1** and a two-dimensional (2D) network structure in **2**. In addition to the assembly structures as well as the geometric and optical isomerism, **1** and **2** showed different SCO properties. SCO properties are affected by the cooperative effect, in which the assembling manner from the building blocks involving geometrical and optical isomerism plays a crucial role for the SCO properties. In particular studies on tetranuclear clusters building up hydrogen bonds like **1** are interesting in making multistep SCO material with thermal hysteresis and in elucidation of SCO mechanisms.

References and Notes

1 a) P. Gütlich, H. A. Goodwin, *Spin Crossover in Transition Metal Compounds I–III* in *Topics in Current Chemistry*, Springer, New York, **2004**, Vol. 233 (doi:10.1007/b40394-9); Vol. 234 (doi:10.1007/b93641); Vol. 235 (doi:10.1007/b96439). b) P. Gütlich, A. Hauser, H. Spiering, *Angew. Chem., Int. Ed. Engl.* **1994**, *33*, 2024. c) J. A. Real, A. B. Gaspar, M. C. Muñoz, *Dalton Trans.* **2005**, 2062. d) M. A. Halcrow, *Chem. Soc. Rev.* **2008**, *37*, 278.

2 a) B. Weber, W. Bauer, J. Obel, *Angew. Chem., Int. Ed.* **2008**, *47*, 10098. b) S. Hayami, K. Hiki, T. Kawahara, Y. Maeda, D. Urakami, K. Inoue, M. Ohama, S. Kawata, O. Sato, *Chem.—Eur. J.* **2009**, *15*, 3497.

3 a) Y. Sunatsuki, Y. Motoda, N. Matsumoto, *Coord. Chem. Rev.* **2002**, *226*, 199. b) I. Katsuki, Y. Motoda, Y. Sunatsuki, N. Matsumoto, T. Nakashima, M. Kojima, *J. Am. Chem. Soc.* **2002**, *124*, 629. c) M. Mimura, T. Matsuo, Y. Motoda, N. Matsumoto, T. Nakashima, M. Kojima, *Chem. Lett.* **1998**, 691.

4 a) Y. Sunatsuki, Y. Ikuta, N. Matsumoto, H. Ohta, M. Kojima, S. Iijima, S. Hayami, Y. Maeda, S. Kaizaki, F. Dahan, J.-P. Tuchagues, *Angew. Chem., Int. Ed.* **2003**, *42*, 1614. b) M. Yamada, H. Hagiwara, H. Torigoe, N. Matsumoto, M. Kojima, F. Dahan, J.-P. Tuchagues, N. Re, S. Iijima, *Chem.—Eur. J.* **2006**, *12*, 4536. c) Y. Ikuta, M. Ooidemizu, Y. Yamahata, M. Yamada, S. Osa, N. Matsumoto, S. Iijima, Y. Sunatsuki, M. Kojima, F. Dahan, J.-P. Tuchagues, *Inorg. Chem.* **2003**, *42*, 7001. d) T. Sato, S. Iijima, M. Kojima, N. Matsumoto, *Chem. Lett.* **2009**, *38*, 178. e) T. Sato, K. Nishi, S. Iijima, M. Kojima, N. Matsumoto, *Inorg. Chem.* **2009**, *48*, 7211. f) H. Hagiwara, S. Hashimoto, N. Matsumoto, S. Iijima, *Inorg. Chem.* **2007**, *46*, 3136. g) Y. Sunatsuki, R. Kawamoto, K. Fujita, H. Maruyama, T. Suzuki, H. Ishida, M. Kojima, S. Iijima, N. Matsumoto, *Inorg. Chem.* **2009**, *48*, 8784. h) Y. Sunatsuki, R. Kawamoto, K. Fujita, H. Maruyama, T. Suzuki, H. Ishida, M. Kojima, S. Iijima, N. Matsumoto, *Coord. Chem. Rev.* **2010**, *254*, 1871. i) K. Nishi, S. Arata, N. Matsumoto, S. Iijima, Y. Sunatsuki, H. Ishida, M. Kojima, *Inorg. Chem.* **2010**, *49*, 1517.

5 ***fac*-[Fe(HL$^{\text{Me-Benz}}$)$_3$]Cl$\cdot$PF$_6$$\cdot$EtOH$\cdot$H$_2$O (1).** To a solution of 2-methyl-4-formylimidazole (0.165 g, 1.5 mmol) in 10 mL of ethanol was added a solution of benzylamine (0.161 g, 1.5 mmol) in 5 mL of ethanol at room temperature. The resulting solution was warmed at 50 °C under stirring for 30 min and then cooled to room temperature. To the ligand solution (1.5 mmol) was added a solution of Fe$^{\text{II}}$Cl$_2$$\cdot$4H$_2$O (0.099 g, 0.5 mmol) in 10 mL of ethanol. To the mixture was added a solution of NaPF$_6$ (0.105 g, 0.5 mmol) in 10 mL of ethanol. The resulting solution was stirred at room temperature for 1 h and filtered. The filtrate was kept for a few days in a refrigerator, during which time large golden-yellow crystals precipitated. They were collected. Yield: 0.22 g. Anal. Calcd for *fac*-[Fe(HL$^{\text{Me-Benz}}$)$_3$]Cl$\cdot$PF$_6$$\cdot$EtOH$\cdot$H$_2$O = C$_{36}H_{39}FeN_9$ClPF$_6$$\cdot$EtOH$\cdot$H$_2$O: C, 50.82; H, 5.27; N, 14.03%. Found: C, 50.74; H, 5.29; N, 13.85%. TGA: 7.1% weight loss was observed. Crystal data: C$_{38}$H$_{47}$FeN$_9$ClPF$_6$O, fw 898.11, cubic, $P\bar{4}3n$ (no. 218), $a = 20.871(3)$ Å, $V = 9091.9(21)$ Å^3, $Z = 8$, $T = 296$ K, $D_{\text{calcd}} = 1.312$ g cm^{-3}, μ(Mo Kα) = 4.92 cm^{-1}, $R = 0.040$ ($I > 2\sigma(I)$), $R_w = 0.112$.

6 ***mer*-[Fe(HL$^{\text{Me-Benz}}$)$_3$]Cl$\cdot$PF$_6$$\cdot$1.5H$_2$O (2).** The ligand was prepared in methanol. To the ligand solution (1.5 mmol) was added a solution of Fe$^{\text{II}}$Cl$_2$$\cdot$4H$_2$O (0.099 g, 0.5 mmol) in 10 mL of methanol. To the mixture was added a solution of NaPF$_6$ (0.105 g, 0.5 mmol) in 10 mL of methanol. The resulting solution was stirred at room temperature for 1 h and filtered. The filtrate was kept for a few days for slow evaporation in air, during which time yellow crystals with small amounts of red crystals precipitated. They were collected by suction filtration. The red crystals were removed by manually and yellow large crystals were collected. Yield: 0.25 g. Anal. Calcd for *mer*-[Fe(HL$^{\text{Me-Benz}}$)$_3$]Cl$\cdot$PF$_6$$\cdot$1.5H$_2$O = C$_{36}H_{39}FeN_9$ClPF$_6$$\cdot$1.5H$_2$O: C, 50.22; H, 4.92; N, 14.64%. Found: C, 50.10; H, 4.86; N, 14.54%. TGA: 3.1% weight loss was observed. Crystal data: C$_{36}$H$_{42}$FeN$_9$ClPF$_6$O$_{1.5}$, fw 861.05, monoclinic, $P2_1/c$ (no. 14), $a = 10.121(3)$ Å, $b = 20.175(6)$ Å, $c = 20.022(5)$ Å, $\beta = 91.023(12)°$, $V = 4087.6(19)$ Å^3, Z = 4, $T = 296$ K, $D_{\text{calcd}} = 1.399$ g cm^{-3}, μ(Mo Kα) = 0.543 cm^{-1}, $R = 0.080$ ($I > 2\sigma(I)$), $R_w = 2.28$. Crystallographic data in the CIF format have been deposited with Cambridge Crystallographic Data Centre: Deposition numbers CCDC-798453 for **1** and CCDC-798454 for **2**.